The Egyptian Journal of Hospital Medicine (July 2024) Vol. 96, Page 2942-2949

Anatomical Variations Detected in Computed Tomography of Paranasal Sinuses

Safa Mohamed Hassan *, Moustafa Mahmoud Abdel Kawi, Shymaa Abdelmawla Shalaby
Radiology Department, Faculty of Medicine, Helwan University, Helwan, Egypt
*** Corresponding author:** Safa Mohamed Hassan, **Email:** safamohamedhasan@gmail.com, **Phone:** +2 01112979438

ABSTRACT

Background: The diseases of the nasal cavity and paranasal sinuses (PNS) are among the most common disorders encountered in clinics of the ear, nose, and throat. Computed tomography (CT) plays an important diagnostic role in patients with sinonasal diseases and determines the treatment.

Objective: To review the anatomical variations of paranasal sinuses and their prevalence detected by computed tomography.

Methods: A cross-sectional study carried out on 185 patients who underwent CT of the nose and PNS. All the studied cases were subjected to CT scanning.

Results: The distribution of the deviated uncinate process among the sides of the nasal cavity showed that 34.5% (19 cases) of cases had it on the right side, 25.5% (14 cases) had it on the left side, and 40% (22 cases) had it bilaterally. Regarding the distribution of maxillary sinus septations, 35.1% (26 out of 74) of cases had bilateral septations, 37.8% (28 out of 74) had septations on the left side, and 27% (20 out of 74) had septations on the right side.

Conclusions: The results underscore the importance of detailed anatomical knowledge, especially for surgical planning in functional endoscopic sinus surgery (FESS). Discrepancies with prior studies were acknowledged, emphasizing the need for further investigation. Overall, the study contributes valuable insights for optimizing patient care and surgical outcomes in otolaryngology.

Keywords: Anatomical Variations, Computed Tomography, Paranasal Sinuses.

INTRODUCTION

Disorders affecting the nasal cavity and paranasal sinuses (PNS) are commonly encountered in clinics specializing in ear, nose, and throat conditions. The frequent presence of anatomical anomalies in this region significantly impacts sinus drainage, often leading to chronic sinusitis [1].

Paranasal sinuses, often referred to as PNS, are air-filled spaces located within specific bones of the skull. There are four pairs of PNS, each named according to the cranial bones where they are situated: the frontal, maxillary, ethmoid, and sphenoid sinuses. Clinically, the PNS can be categorized into two distinct groups: the anterior and posterior groups. The anterior group includes the maxillary, frontal, and anterior ethmoidal air cells, while the posterior group consists of the posterior ethmoidal and sphenoidal air cells [2].

Preoperative imaging is crucial for evaluating the structures surrounding the PNS. By assessing anatomical features such as the carotid artery and optic nerve, surgeons can identify critical areas for surgical intervention and anticipate potential complications. Imaging techniques provide precise and detailed visualization of these key structures from the surgeon's perspective. With the advent of CT imaging, previously unexplored aspects of sinonasal diseases and variations in the osteomeatal complex (OMC) can now be thoroughly examined [1].

Recognizing the clinical and surgical importance of anatomical variations in the PNS is essential. Certain anatomical variations are believed to contribute to sinus problems, making it imperative for radiologists to be familiar with these variations, especially when the patient is a candidate for functional endoscopic sinus surgery (FESS) [3].

Computed tomography (CT) plays a vital role in diagnosing sinonasal diseases and determining the most appropriate treatment. CT images provide an accurate depiction of the intricate structural composition of the bones, enabling the identification of anatomical variations, assessment of disease severity, and classification of various inflammatory, benign, and malignant sinonasal conditions. CT is the preferred imaging modality for evaluating congenital, inflammatory, benign, and malignant diseases in the sinonasal region. Additionally, it is used to assess related complications and guide subsequent medical interventions [4].

CT generates high-resolution images that offer precise details of the structures under investigation. In endodontic therapy, CT scans can enhance surgical treatment planning by providing accurate information about the size and location of lesions in relation to nearby anatomical structures. CT has become the leading technique in medicine for visualizing the maxillary sinuses, as it provides detailed images of both bone and soft tissue from multiple angles using thin sections [5].

The aim of this work was to review the anatomical variations of PNS and their prevalence detected by CT.

PATIENTS AND METHODS

This a cross-sectional study carried out on 185 patients who underwent CT of the nose and PNS. They were selected from the Department of Radiology, Helwan University Hospital [Badr Hospital] during the period from 1st November 2022 to June 2023 (8 months duration).

Received: 26/02/2024
Accepted: 25/04/2024

Inclusion criteria were age 18-77 years, both male and female patients and patients who had CT scans on the nose and paranasal sinuses for various forms of pathology.

Exclusion criteria were all postoperative cases and patients with any traumatic conditions involving PNS, with sinonasal neoplasms and below 18 years old.

All the studied cases were subjected to CT scanning:

Axial, coronal and sagittal images were acquired using multi-detector CT unit. All sinuses (frontal, maxillary, ethmoid and sphenoid) were assessed for pattern of aeration, location, expansion of sinuses and anatomical variants. The CT examination was performed with Toshiba Aquilion prime 128 slice Helical Computed tomography machine. The coronal section slice thickness was 2.25 mm. The section extended from the anterior region of the frontal sinus to the posterior region of the sphenoid sinus. The kilovolt peak (KVP) was set to 120, the milliampere-seconds (mAs) to 150, and the scan time to 5 seconds.

Each patient's lateral nasal wall was examined for anatomical variations in the osteomeatal complex (OMC), including concha bullosa, paradoxical middle turbinate, Agger nasi cell, Haller cell, uncinate process deviation, and nasal septal anomalies. The study also recorded structural variations in the olfactory fossae, specifically measuring the depth of the olfactory fossa according to Keros' classification, as well as noting any irregularities in the height and configuration of the ethmoid roof. Additional anatomical variations observed included the presence of Onodi cells, absence of the frontal sinus, presence of septations in the maxillary sinus, and underdevelopment of the maxillary sinus.

The CT exams focused on studying the structure of the ethmoid sinus roof, particularly to identify any variations in height and the presence of curvature in the lateral lamella of the cribriform plate. "Angulation" refers to an increase in the angle between the lateral lamella and the horizontal part of the cribriform plate. The depth of the olfactory fossa was determined by measuring the height of the lateral lamella and classified into types I, II, or III according to the Keros classification [6].

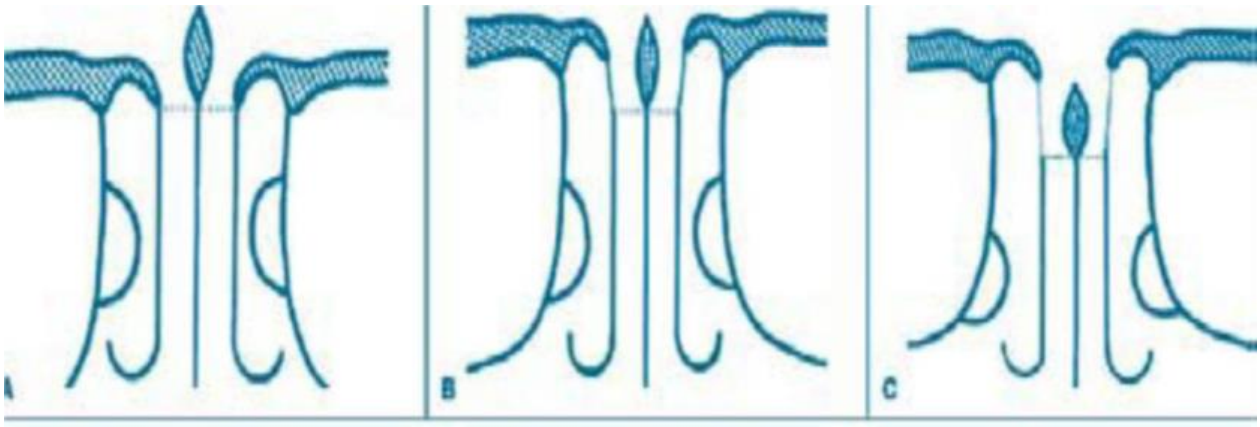

Figure 1: Schematic representation of three types of the olfactory fossa according to Keros classification: A, type I; B, type II; C, type III.

Coronal images were used to determine the position of the cribriform plate and ethmoid roof in relation to the orbital floor, as indicated by the infraorbital nerve, which is easily identifiable on a coronal CT scan. Two reference points were selected at the base of the skull: the medial ethmoid roof point (MERP), corresponding to the junction between the medial ethmoid roof and the lateral lamella of the cribriform plate, and the lowest position of the cribriform plate (CP). In each image, measurements were taken for the distance between the MERP and the horizontal plane, as determined by the infraorbital nerve (referred to as the MERP height), and the distance between the CP and the horizontal plane, also determined by the infraorbital nerve (referred to as the CP height). The length of the lateral lamella of the cribriform plate (LLCP) was calculated by subtracting the height of the cribriform plate (CP) from the height of the medial ethmoid roof point (MERP) (LLCP = MERP height - CP height). The length of the LLCP was measured in each image using the Keros classification. Additionally, the depths of the olfactory fossae on both sides were compared [7].

Each CT scan was interpreted separately by two senior radiologists, when there was difference in interpreting of the CT scans, the interpretation was done by consensus of the 2 physicians.

Ethical considerations

The study was done after being accepted by the Research Ethics Committee, Helwan University (Serial no: 86-2022). All patients provided written informed consents prior to their enrolment. The consent form explicitly outlined their agreement to participate in the study and for the publication of data, ensuring protection of their confidentiality and privacy. This work has been carried out in accordance with The Code of Ethics of the World Medical Association (Declaration of Helsinki) for studies involving humans.

Statistical analysis

The statistical analysis was conducted using SPSS version 28 (IBM, Armonk, New York, USA). The qualitative data were expressed in terms of frequency and percentage. The quantitative data were displayed using measures such as the mean, standard deviations, median, and range.

RESULTS

Table 1 shows demographic data of the studied cases and characteristics of cases with absent frontal sinuses and with concha bullosa.

Table 1: Demographic data of the studied cases and characteristics of cases with absent frontal sinuses and with concha bullosa

Variable		**Total cases (n=185)**	**Cases with absent frontal sinuses (n=17)**	**Cases with Concha bullosa (n=120)**
Age (years)	Mean ± SD	47.2±18.8	49.4±18.4	45±19.4
Age groups, n (%)	<40	73(39.5%)		
	40-60	56(30.3%)		
	>60	56(30.3%)		
Gender, n (%)	Female	67(36.2%)	10(58.8%)	42(35%)
	Male	118(63.8%)	7(41.2%)	78(65%)
Distribution, n (%)	Bilateral	----	6(35.3%)	74(61.7%)
	Left	----	2(11.8%)	20(16.7%)
	Right	----	9(52.9%)	26(21.7%)

Table 2 shows different patterns of concha bullosa in the studied cases and characteristics of cases with paradoxical middle turbinates.

Table 2: Different patterns of concha bullosa in the studied cases and characteristics of cases with paradoxical middle turbinates

Variable		**Total cases (n=120)**
Different patterns of concha bullosa, n (%)	True concha bullosa	31(25.8%)
	Lamellar type	77(64.2%)
	Bulbous type	12(10.0%)
Cases with Paradoxical middle turbinates		Total cases (n=30)
Age (years)	Mean ± SD	43.4±22.6
Gender, n (%)	Female	15(50%)
	Male	15(50%)
Distribution, n (%)	Bilateral	11(36.7%)
	Left	13(43.3%)
	Right	6(20%)

Table 3 shows characteristics of cases with Agger nasi cell, Haller cell, Onodi cell and deviated uncinate process**.**

Table 3: Characteristics of cases with Agger nasi cell, Haller cell, Onodi cell and deviated uncinate process

Variable		Total cases (n=181)
Age (years)	Mean ± SD	46.2±19.3
Gender, n (%)	Female	63(34.8%)
	Male	118(65.2%)
Distribution, n (%)	Bilateral	130(71.8%)
	Left	25(13.8%)
	Right	26(14.4%)
Cases with Haller cell		Total cases (n=78)
Age (years)	Mean ± SD	44.8±21.2
Gender, n (%)	Female	23(29.5%)
	Male	55(70.5%)
Distribution, n (%)	Bilateral	32(41%)
	Left	18(23.1%)
	Right	28(35.9%)
Cases with Onodi cell		Total cases (n=20)
Age (years)	Mean ± SD	49.2±18
Gender, n (%)	Female	8(40%)
	Male	12(60%)
Distribution, n (%)	Bilateral	8(40%)
	Left	6(30%)
	Right	6(30%)
Cases with deviated uncinate process		Toral cases (n=55)
Age (years)	Mean ± SD	45.1±21.9
Gender, n (%)	Female	21(38.2%)
	Male	34(61.8%)
Distribution, n (%)	Bilateral	22(40%)
	Left	14(25.5%)
	Right	19(34.5%)

Table 4 shows characteristics of cases with nasal septum deviation, nasal septal spur, and chondrovomerine deformation.

Table 4: Characteristics of cases with nasal septum deviation, **nasal septal spur**, **and chondrovomerine deformation**

Variable		Toral cases (n=107)
Age (years)	Mean ± SD	49.2±17.3
	Median (Range)	50(17-77)
Gender, n (%)	Female	35(32.7%)
	Male	72(67.3%)
Distribution, n (%)	Left	37(34.6%)
	Right	70(65.4%)
Cases with nasal septal spur		Toral cases (n=12)
Age (years)	Mean ± SD	49.8±6
Gender, n (%)	Female	4(33.3%)
	Male	8(66.7%)
Distribution, n (%)	Left	5(41.7%)
	Right	7(58.3%)
Cases with chondrovomerine deformation		Toral cases (n=6)
Age (years)	Mean ± SD	51.4±4
Gender, n (%)	Female	4(66.7%)
	Male	2(33.3%)

Table 5 shows characteristics of cases with maxillary sinus septations, maxillary sinus hypoplasia and distribution of olfactory fossa according to side and Keros classification.

Table 5: Characteristics of cases with maxillary sinus septations, maxillary sinus hypoplasia and distribution of olfactory fossa according to side and Keros classification

Variable		Total cases (n=74)	
Age (years)	Mean ± SD	49.2±19.6	
	Median (Range)	50(17-76)	
Gender, n (%)	Female	37(50%)	
	Male	37(50%)	
Distribution, n (%)	Bilateral	26(35.1%)	
	Left	28(37.8%)	
	Right	20(27%)	
Cases with maxillary sinus hypoplasia		Total cases (n=11)	
Age (years)	Mean ± SD	44.4±19.9	
Gender, n (%)	Female	3(27.3%)	
	Male	8(72.7%)	
Distribution, n (%)	Bilateral	9(81.8%)	
	Left	0(0%)	
	Right	2(18.2%)	
Distribution of olfactory fossa: Total cases (n=185)		Right side	Left side
Keros classification, n (%)	Keros I	115(62.2%)	130(70.3%)
	Keros II	70(37.8%)	55(29.7%)
	Keros III	0(0%)	0(0%)

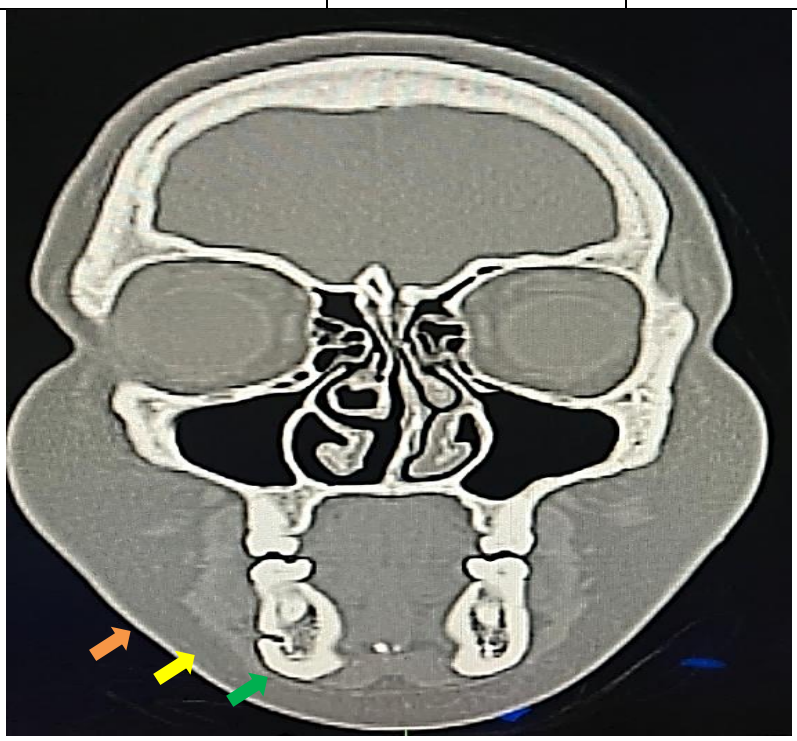

Figure 2: Coronal CT scan showing right concha bullosa (yellow arrow), right Haller cell (orange arrow) and slightly deviated nasal septum to the left (green arrow).

DISCUSSION

CT imaging assumes a pivotal role in preoperative assessments by providing indispensable insights into adjacent anatomical structures, such as the optic nerve and carotid artery. This modality aids in surgical planning by illuminating critical loci for intervention and mitigating the risk of intraoperative complications [8].

In terms of demographic data, the studied patients had a mean age of 47.2±18.8 years. The frequency of age distribution showed that (39.5%) were under the age of 40, (30.3%) between the ages of 40 and 60, and (30.3%) over the age of 60. In terms of gender, out of the total cases, (36.2%) were females and (63.8%) were males. Similarly, **Devaraja *et al.*** performed a study to evaluate the structural variations in CT scans of paranasal sinuses and investigate any potential relationships among them. The investigation was carried out retrospectively at a tertiary care medical center situated in southern India [9].

In our study, out of the 17 cases with absent frontal sinuses, which accounted for 9.2% of the total cases, their mean age was 49.4±18.4 years. The median age was 50 years, with a range of 18 to 77 years. In terms of gender distribution, 10 cases (58.8%) were females, while 7 cases (41.2%) were males. Regarding the distribution of absent frontal sinuses, 6 cases (35.3%) were bilateral, 2 cases (11.8%) were on the left side, and 9 cases (52.9%) were on the right side.

In harmony with our results, **Assiri and Alroqi** conducted a study using CT scans of the paranasal sinuses to investigate the prevalence of frontal sinus aplasia in the Saudi Arabian population. An extensive examination was carried out on a grand total of 449 patients. Among the entire population, there were 226 males, accounting for 50.3% of the total, and 223 females, making up 49.7% of the total. The mean age of all the participants was 39.15 years. A total of 15 patients, accounting for 3.3% of the total, were diagnosed with bilateral frontal sinus agenesis. A total of 23 instances, representing 5.1% of the total, exhibited right aplasia, whereas 6 cases, accounting for 1.3% of the total, exhibited left aplasia. Multiple studies, including the present one, have shown that females have a higher prevalence of both bilateral and unilateral absence of the frontal sinus [10].

In the current work, out of the 120 cases with concha bullosa, which accounted for 64.9% of the total cases, their mean age was 45±19.4 years. In terms of gender distribution, 42 cases (35%) were females and 78 cases (65%) were males. The distribution of concha bullosa among the sides of the nasal cavity showed that 74 cases (61.6%) had it bilaterally, 20 cases (16.7%) had it on the left side, and 26 cases (21.7%) had it on the right side.

In line with our research, **El-Din *et al.*** investigated the prevalence of CB in the adult population of Saudi Arabia and its association with sinusitis using multidetector CT. The number of males was 540, whereas the number of females was 339. We eliminated patients with face congenital deformities or nasal injuries from our investigation. A Lightspeed VCT 64 slice CT equipment was utilized to conduct a multidetector CT scan [11].

Among the CT scans analyzed for the nose and paranasal sinuses (PNS) of 202 patients, the incidence of CB was found to be 31.7%. Concha bullosa was seen bilaterally in 35 individuals, accounting for 54.7% of the total, whereas it was found unilaterally in 29 patients, representing 45.3% of the total. Among the 99 cases of CB, 54 (54.5%) were located on the right side, whereas 45 (45.5%) were located on the left side. Two patients presented with mucopyocele in the lamellar portion of the CB, while four patients exhibited significant mucosal thickening across the CB.

In our study, according to paradoxical middle turbinates, which constituted 16.2% of the total cases (30 cases), their mean age was 43.4±22.6 years. In terms of gender distribution, 15 cases (50%) were females and 15 cases (50%) were males. The distribution of paradoxical middle turbinates among the sides of the nasal cavity showed that 6 cases (20%) had it on the right side, 13 cases (43.3%) had it on the left side, and 11 cases (36.7%) had it bilaterally.

A paradoxical middle turbinate is defined by the anomalous inward concavity of the middle turbinate, irrespective of its effect on the middle meatus. Our analysis corroborates the findings of **Shalini and Gopal,** which indicate that out of the 100 individuals investigated, 12 displayed paradoxical curvature of the middle turbinate. Out of these cases, 7 were male and 5 were female. The incidence of this phenomenon was greater in females (13.16%) compared to males (11.29%), although this disparity did not achieve statistical significance (p=0.780). Unilateral paradoxical middle turbinate was more prevalent than bilateral (4%), although the difference was not statistically significant (p=0.679) [12].

In our study, regarding Agger nasi cell presence, 181 cases were found which comprised 97.8% of studied cases, their mean age was 46.2±19.3 years. In terms of gender distribution, 34.8% were females and 65.2% were males. The distribution of Agger nasi cell among the sides of the nasal cavity showed that 13.8% of cases had it on the left side, 14.4% had it on the right side, and 71.8% had it bilaterally.

The reported prevalence in different series ranges from 88.5% as reported by **Maru and Gupta**. to nearby all as reported by **Zinreich *et al.*, and Pérez-piñas *et al.*** [13-15].

In our study, out of 55 cases with a deviated uncinate process which accounted 29.7% of cases, their mean age was 45.1±21.9 years. In terms of gender distribution, 38.2% (21 cases) were females and 61.8% (34 cases) were males. The distribution of the deviated uncinate process among the sides of the nasal cavity showed that 34.5% (19 cases) of cases had it on the right

side, 25.5% (14 cases) had it on the left side, and 40% (22 cases) had it bilaterally.

Tuli *et al.* carried out a study on a group of 50 persons who were diagnosed with chronic sinusitis. The study specifically examined the uncinate processes of 100 patients. The experiment consisted of a cohort of 50 individuals who had been diagnosed with chronic sinusitis and had failed to show improvement after a 2-week course of medical treatment. The patients demonstrated a willingness to undergo endoscopic sinus surgery and CT scanning of the PNS. The patient had diagnostic nasal endoscopy and CT scanning of the paranasal sinuses, including both coronal and axial sections, to assess the structure and deviations of the uncinate process [16].

In our study, nasal septum deviation was represented in 57.8% of cases (107 cases), their mean age of the 107 cases with nasal septum variations is 49.2±17.3 years, with a median age of 50 years and a range of 17 to 77 years. In terms of gender distribution, 35 individuals (32.7%) with nasal septum variations were female and 72 individuals (67.3%) were male. Regarding the distribution of these variations, 37 cases (34.6%) were on the left side and 70 cases (65.4%) were on the right side.

Our findings regarding prevalence of deviated nasal septum, gender distribution, and direction of deviation are different from the findings of **Sumaily *et al.*** Cases were investigated with CT and they had no previous history of sinonasal surgeries. The Lund Mackay staging system was used to assess the OMC and all PNS disease staging if present [17].

In our study, according to cases with maxillary sinus septations (n=74, 40% of total cases), their mean age was 49.2±19.6 years. The gender distribution revealed that 50% (37 out of 74) were females and 50% (37 out of 74) were males. Regarding the distribution of maxillary sinus septations, 35.1% (26 out of 74) of cases had bilateral septations, 37.8% (28 out of 74) had septations on the left side, and 27% (20 out of 74) had septations on the right side.

Alhumaidan *et al.* conducted a study to investigate the prevalence of maxillary sinus septa and its correlation with age, gender, dental condition, and the probability of perforating the Schneiderian membrane. Their analysis involved the utilization of cone beam computed tomography (CBCT). A total of 178 CBCT images, which included 356 sinuses, were evaluated. The demographic data, including age and sex, were collected from the recorded information in the CBCT program prior to performing the procedure. The sample consisted of 100 men and 78 females, resulting in a male-to-female ratio of 1.3 to 1 [18].

Our analysis revealed that most patients exhibited Keros type I classification in terms of the distribution of depths in the olfactory fossa. More precisely, this categorization was observed in 62.2% of instances on the right side and 70.3% of instances on the left side. The Keros type II classification was present in 37.8% of instances on the right side and 29.7% of cases on the left side. No occurrences of Keros type III classification were discovered on either side.

Almushayti *et al.* conducted a cross-sectional study to evaluate the prevalence of various types of Keros and their frequency by analyzing the depth of the olfactory fossa (OF) using the Keros classification on PNS CT scans in the Qassim region [19].

This was a single-center study with a relatively small sample size, which might limit the generalizability of the findings to a larger population. The study's age distribution was skewed towards middle-aged individuals, possibly affecting the representation of anatomical variations prevalent in younger or older age groups. Excluding postoperative cases, traumatic conditions, and sinonasal neoplasms might have eliminated specific cases with unique anatomical variations associated with these conditions.

CONCLUSION

In this study by assessing PNS anatomical variations through CT scans in 185 patients, diverse findings were revealed. Variations such as concha bullosa, paradoxical middle turbinates, Agger nasi cell, Haller cell, Onodi cell, deviated uncinate process, deviated nasal septum, maxillary sinus septations, maxillary sinus hypoplasia, and olfactory fossa depth were analyzed in terms of prevalence and distribution. The results underscore the importance of detailed anatomical knowledge, especially for surgical planning in FESS. Discrepancies with prior studies were acknowledged, emphasizing the need for further investigation. Overall, the study contributes valuable insights for optimizing patient care and surgical outcomes in otolaryngology.

Financial support and sponsorship: Nil.
Conflict of Interest: Nil.

REFERENCES

1. **Kaya M, Çankal F, Gumusok M *et al.* (2017)**: Role of anatomic variations of paranasal sinuses on the prevalence of sinusitis: Computed tomography findings of 350 patients. Niger J Clin Pract., 20:1481-8.
2. **Ribeiro B, Muniz B, Marchiori E (2019)**: Preoperative computed tomography evaluation of the paranasal sinuses: what should the physician know? - pictorial essay. Radiol Bras., 52:117-22.
3. **Jaworek-Troć J, Zarzecki M, Mróz I *et al.* (2018)**: The total number of septa and antra in the sphenoid sinuses - evaluation before the FESS. Folia Med Cracov., 58:67-81.
4. **Kandukuri R, Phatak S (2016)**: Evaluation of sinonasal diseases by computed tomography. J Clin Diagn Res., 10:Tc09-tc12.
5. **Qureshi M, Usmani A (2020)**: Clinically significant variation of paranasal sinuses on CT-scan. Journal of

Bahria University Medical and Dental College, 10:152-7.

6. **Souza S, Souza M, Idagawa M *et al.* (2008)**: Computed tomography assessment of the ethmoid roof: a relevant region at risk in endoscopic sinus surgery. Radiologia Brasileira, 41:143-7.
7. **Solares C, Lee W, Batra PS *et al.* (2008)**: Lateral lamella of the cribriform plate: software-enabled computed tomographic analysis and its clinical relevance in skull base surgery. Archives of Otolaryngology–Head & Neck Surgery, 134:285-9.
8. **Zhao Y, Bao D, Wang X *et al.* (2022)**: Prediction model based on preoperative CT findings for carotid artery invasion in patients with head and neck masses. Front Oncol., 12:987031.
9. **Devaraja K, Doreswamy S, Pujary K *et al.* (2019)**: Anatomical variations of the nose and paranasal sinuses: A computed tomographic study. Indian J Otolaryngol Head Neck Surg., 71:2231-40.
10. **Assiri K, Alroqi A (2021)**: Frequency of the frontal sinus aplasia among Saudi Arabian population. A single-center retrospective case review. Saudi Med J., 42:228-31.
11. **El-Din W, Madani G, Fattah I *et al.* (2021)**: Prevalence of the anatomical variations of concha bullosa and its relation with sinusitis among Saudi population: a computed tomography scan study. Anat Cell Biol., 54:193-201.
12. **Shalini S, Gopal T (2018)**: Paradoxical curvature of middle turbinate: A computed tomographic study. International Journal of Contemporary Medical Research, 5:2454-7379.
13. **Maru Y, Gupta V (2001)**: Anatomic variations of the bone in sinonasal C.T. Indian J Otolaryngol Head Neck Surg., 53:123-8.
14. **Zinreich S, Kennedy D, Rosenbaum A *et al.* (1987)**: Paranasal sinuses: CT imaging requirements for endoscopic surgery. Radiology, 163:769-75.
15. **Pérez-Piñas I, Sabaté J, Carmona A *et al.* (2000)**: Anatomical variations in the human paranasal sinus region studied by CT. J Anat., 197 (Pt 2):221-7.
16. **Tuli I, Sengupta S, Munjal S *et al.* (2013)**: Anatomical variations of uncinate process observed in chronic sinusitis. Indian J Otolaryngol Head Neck Surg., 65:157-61.
17. **Sumaily I, Hudise J, Aldhabaan S (2017)**: Relation between deviated nasal septum and paranasal sinus pathology. Int J Otorhinolaryngol Head Neck Surg., 3:786.
18. **Alhumaidan G, Eltahir M, Shaikh S (2021)**: Retrospective analysis of maxillary sinus septa - A cone beam computed tomography study. Saudi Dent J., 33:467-73.
19. **Almushayti Z, Almutairi A, Almushayti M *et al.* (2022)**: Evaluation of the Keros classification of olfactory fossa by CT scan in Qassim Region. Cureus, 14:e22378.